Order–disorder transitions in Langmuir–Blodgett films. III. Polarized Raman studies of cadmium arachidate using integrated optical techniques

J. P. Rabe,[a] J. D. Swalen, and J. F. Rabolt
IBM Research, Almaden Research Center, San Jose, California 95120-6099

(Received 17 October 1986; accepted 23 October 1986)

Polarized Raman measurements of Langmuir–Blodgett (LB) multilayers of cadmium arachidate (CdA) have been obtained through the application of integrated optical techniques. Excitation of either the transverse electric (TE) or transverse magnetic (TM) mode of an asymmetric slab waveguide was alternately used to produce Raman scattering in the CdA multilayers deposited on its surface. Analysis of the 90° scattered light with a polarizer placed at two mutually perpendicular positions for both the TE and TM modes of the waveguide produced a set of four measurements which were used to determine the orientation and lateral order of the CdA monolayer components. The extent of order in the LB film was then investigated as a function of temperature and compared with that of bulk CdA. The temperature of the order–disorder transition was found to be similar in both cases and consistent with that found previously from infrared studies.

I. INTRODUCTION

With continued interest in the use of thin films as both active and passive components in microelectronic devices there has been an increasing realization that conventional methods for the characterization of these structures were inadequate. Thus, recently there has been a resurgence of novel experimental techniques specifically designed to investigate molecular structure in the submicron regime. Waveguide Raman spectroscopy (WRS) is one of the techniques currently used to study thin films which has evolved over the past decade. Studies by Levy *et al.*[1,2] indicated that a thin film supported on a substrate of lower refractive index forming an asymmetric slab waveguide could be used to obtain a Raman spectrum. Due to considerable spectral interference attributable to the substrate, Raman studies of thin films were limited to those whose minimum thicknesses approached 1–2 μ. This technique was later placed on a firm basis[3,4] when the Raman spectrum of a 1 μ polymer film was obtained. The success was attributed to the use of selected substrates having a much lower refractive index. Subsequent progress[4] into the submicron regime occurred shortly thereafter by the choice of a four layer waveguide system containing a "guiding layer" permanently deposited on the substrate whose sole function was to trap and guide light along the top of the substrate. It was the evanescent field emanating from the waveguide which excited Raman scattering from the thin film deposited on its surface. There were no restrictions on the thickness of the film whose Raman spectrum was desired and isotropic films as thin as 800 Å were studied.[4]

Langmuir–Blodgett films are an extremely attractive candidate for investigation by WRS. These two-dimensionally oriented films can be deposited on waveguide structures and explored via polarized light. The evanescent field from the guiding layer is highly polarized depending on whether a transverse electric (TE) or transverse magnetic (TM) mode of the waveguide has been selected. This polarized light can be used to explore the anisotropic character of LB films, determining information about both the orientation and lateral order of molecules. This work reports such studies with their subsequent extension to elevated temperatures. An order–disorder transition has been observed in the two-dimensional LB films of CdA and compared to the kinetics of a similar transition observed in bulk CdA. The extent of inter- and intramolecular order has been characterized as a function of temperature and has provided an insight into the mechanism of defect introduction at elevated temperatures.

II. EXPERIMENTAL

A. Langmuir–Blodgett films

Arachidic acid was used as received from Lachat Chemical, Inc. The LB films were prepared on a commercially available film balance (Joyce–Loebel), which had been modified by replacing the originally supplied glass tank with a solid Teflon trough. The subphase was purified water (Barnstead nanopure) containing 2.5×10^{-4} mol/ℓ $CdCl_2$ and Na_2CO_3 to maintain a *p*H between 7.0 and 7.5 Monolayers of the cadmium salt of arachidic acid (CdA) were transferred on glass waveguides (Corning 7059 glass sputtered on quartz or Pyrex) at a dipping speed of about 3 mm/min and a pressure of 30 mN/m.

B. Waveguide assembly

Raman measurements were made on multilayered (13-55) LB films of CdA using the scattering geometry schematically shown in Fig. 1. The incident laser was coupled into the waveguide assembly (magnified in lower part of Fig. 1) by a high index glass prism (Schott LaSF5) in order to insure that a large range of wave vectors, **k**, were available for coupling.[2–6] The prism was clamped against the film by both a single and double stage[7] coupling device; the latter was required for elevated temperature studies so as to avoid cou-

[a] Present address: Max-Planck-Institut für Polymerforschung, Postfach 3148, D-6500 Mainz, West Germany.

 0021-9606/87/031601-07$02.10

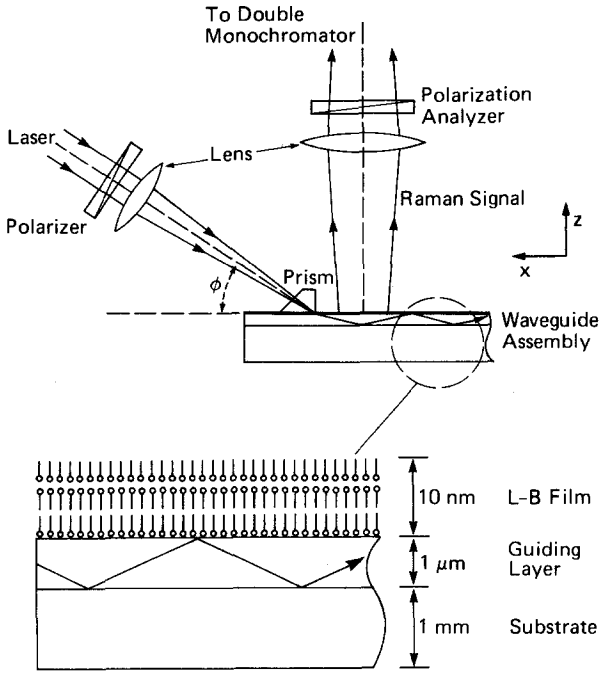

FIG. 1. Schematic of WRS scattering geometry and waveguide structure used for studies of LB films.

pling losses due to the inherent expansion of the metal coupling assembly at high temperatures.[7] As has been discussed previously,[3,8] the thin film assembly will conduct light only for certain coupling angles, ϕ, which correspond to discrete solutions of an eigenvalue equation derived from Maxwell's equations with the appropriate boundary conditions for a four layer asymmetric slab waveguide. For these values of ϕ, the light will propagate in the guiding layer (GL) and perhaps also in the LB film depending on the refractive index difference between the two layers. In the event that laser light is trapped in the 1 μ thick guiding layer as is illustrated in Fig. 1, then an evanescent or guided wave exists within the surface deposited film and will give rise to Raman scattering from the deposited multilayer components.

Whether the light field within the deposited layer is evanescent or guided is determined by its refractive index. Since each mode of the GL has an effective refractive index, n_{eff}, in the range between that of the bulk and substrate, then if the index of the adsorbed layer, n_A, is higher than n_{eff} of a specific mode, the mode will be guiding in both layers. Conversely if n_A is less than n_{eff} the wave is evanescent in the adsorbed layer. Frequently for some of the lower ($m = 0,1$) modes, the field is evanescent while for higher ($m = 2,3,4$) modes it is guiding as in the case for polymer laminates studied previously.[9]

C. Raman spectroscopy

All Raman measurements were made using the right angle scattering geometry depicted in Fig. 1. Spectra were recorded using a Jobin–Yvon HG-2S double monochromator equipped with a cooled RCA 31034A-02 photomultiplier tube and standard photon counting electronics. All data were collected and processed with a Nicolet 1180 data system. Sample illumination was provided by Spectra Physics 165-08 and 2020 argon ion lasers. Typical Raman measurements were made using the 488.0 nm line with a spectral resolution of 4 or 8 cm^{-1}.

III. RESULTS AND DISCUSSION

A. Bulk cadmium arachidate

Cadmium arachidate is possibly one of the most highly investigated materials[10–16] in the form of LB films but, surprisingly, little work has been concerned with its structure in the bulk. Early x-ray studies[17] on CdA powder as a function of temperature indicated the presence of three condensed phases. The first phase exists from room temperature to 110 °C and consists of a periodic lamellar structure with the planes of cadmium atoms separated by a crystalline bilayer of hydrocarbon chains in a simple bilayered structure. The second phase existed up to ~220 °C and was characterized as the principal mesomorphic phase with the cylindrical elements packed in a two-dimensional hexagonal array similar to a liquid state. In this phase, considerable disorder of the hydrocarbon chain was thought to occur as was reflected in a lowering of the d spacing corresponding to the length of the chain. Finally, the high temperature phase $T > 220°$ was found to coexist over only a short temperature range (20°) and differed from the previous only in the observed low angle x-ray scattering long spacing.

Spectroscopic studies of bulk CdA have also been rare. IR spectra of CdA powder were initially recorded[11] to compare the results with those obtained from LB multilayers but no detailed analysis of the observed bands was made.

The room temperature Raman spectrum of CdA powder is shown in Fig. 2. In the 1600–1000 cm^{-1} region are found a number of strong bands which can be assigned based on analogous measurements which have been made on n-alkanes.[18] The strong bands at 1060 and 1130 cm^{-1} correspond to the asymmetric, ν_a (CC), and symmetric, ν_s (CC), carbon–carbon stretching vibrations, respectively. The intense band found at 1295 cm^{-1} is attributable to the CH_2 twisting vibration, $t(CH_2)$. A series of three bands are found in the 1400–1500 cm^{-1} region. The bands at 1460 and 1440 cm^{-1} have been alternately assigned[19–21] to a CH_2 bending vibration. The remaining band at 1415 cm^{-1} has been attributed to an overtone of the IR active CH_2 rocking vibration

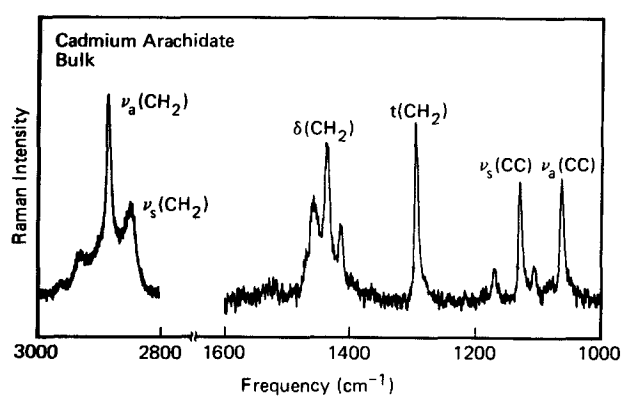

FIG. 2. Room temperature Raman spectrum of bulk CdA. Bands of interest are labeled as ν_a—asymmetric stretch, ν_s—symmetric stretch, δ—bend, and t—twist.

in Fermi resonance with one of the remaining bands in this region. The Raman band at 1415 cm^{-1} only appears when the unit cell has orthorhombic symmetry.[21] In addition, the relative peak heights and half-widths of the $\nu_a(CH_2)$ and $\nu_s(CH_2)$ stretching vibrations found in the 2800–3000 cm^{-1} region also are indicative of an orthorhombic subcell structure.[19] These observations are consistent with the crystal field splittings observed in the IR spectrum of bulk CdA.[11]

B. LB films of cadmium arachidate

As indicated previously, the scattering geometry used to obtain polarized Raman measurements from the LB multilayers of CdA is shown in Fig. 1. In the laboratory frame of reference the incident laser propagates along the $-X$ direction while the scattered light is viewed along the Z direction. The incident light can be polarized either along the Z or Y direction while an analyzer for the scattered light can be placed parallel to either the X or Y axis.

Shown in Fig. 3 are the polarized Raman spectra of CdA multilayers. The designation for each Raman spectrum describing the incident polarization and the direction of the analyzer is due to Damen *et al.*[22] It is of the form $A(BC)D$, where A and D are the propagation directions of the incident (A) and scattered (D) radiation, while B and C refer to the direction of polarization of the incident (B) and analyzed (C) radiation, respectively. Thus in the top spectrum of Fig. 3 the incident beam propagates along the laboratory X axis with polarization parallel to Y. The scattered radiation was viewed along Z through a polarizer aligned parallel to the laboratory Y axis.

The broad features underlying the spectra of Fig. 3 are due to the high index guiding layer deposited on the substrate. Most likely these correspond to fluorescent features due to the presence of impurities in the glass combined with Raman scattering from the amorphous glass itself. As shown in Fig. 4 the CH stretching region does not contain any noticeable background contribution from the glass to either the $X(YY)Z$ or the $X(YX)Z$ spectra.

Perhaps the simplest means of analyzing the polarization data is to draw upon results obtained in previous IR studies[11] which concluded that the subcell symmetry of the CH_2 groups was orthorhombic in LB multilayer films of CdA. The orthorhombic subcell symmetry of the CH_2 groups occurs for both an orthorhombic and monoclinic macrocell containing a bilayer assembly. In the former case, the chains would be oriented normal to the surface plane of the bilayer; in the latter the chains would be tilted at an angle of 61° relative to this plane as indicated previously.[11] IR dichroic measurements of chain orientation in LB films of CdA indicate that the hydrocarbon tails are oriented very close[13] to normal to the surface suggesting that both the subcell and the macrocell are orthorhombic.[11] Recent electron diffraction studies[23] on CdA multilayers support this conclusion. Since this is the case, an analysis of the observed Raman data can be carried out in terms of the D_{2h} symmetry of the subcell according to Snyder.[24] For the scattering geometry shown in Fig. 1, the following polarization experiments will give:

Experiment	Symmetry species	Polarizability contributions
$X(YY)Z$	$A_g + B_{1g}$	$\frac{1}{8}[2(\alpha_{xx}+\alpha_{yy})^2 + (\alpha_{xx}-\alpha_{yy})^2] + \frac{1}{2}\alpha_{xy}^2$
$X(YX)Z$	$A_g + B_{1g}$	$\frac{1}{8}(\alpha_{xx}-\alpha_{yy})^2 + \frac{1}{2}\alpha_{xy}^2$
$X(ZY)Z$	$B_{2g} + B_{3g}$	$\frac{1}{2}\alpha_{zx}^2 + \frac{1}{2}\alpha_{yz}^2$
$X(ZX)Z$	$B_{2g} + B_{3g}$	$\frac{1}{2}\alpha_{xz}^2 + \frac{1}{2}\alpha_{yz}^2$.

It is important to realize at this point that the particular scattering geometry afforded by WRS is unique and is more difficult to achieve in single crystals of n-paraffins and oriented specimens of polyethylene since it would require orienting the chain axis along the Z direction (the optic axis of

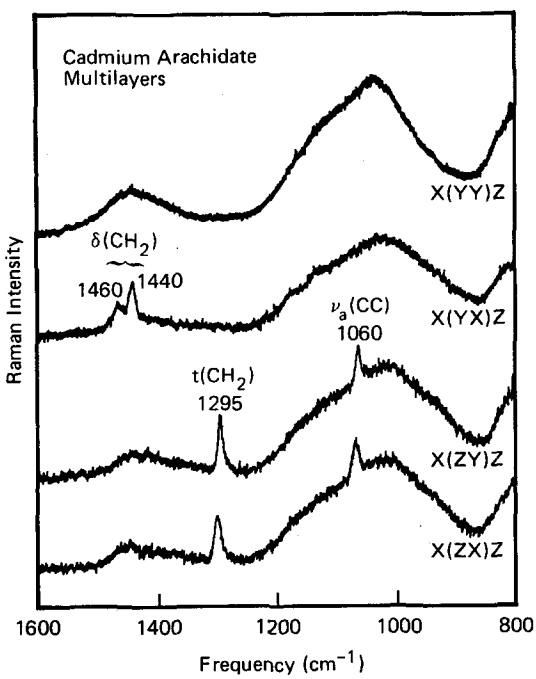

FIG. 3. Polarized Raman measurements (1600–800 cm^{-1}) of 13 multilayers of CdA. Polarization notation for each experiment is that of Damen *et al.* (Ref. 24).

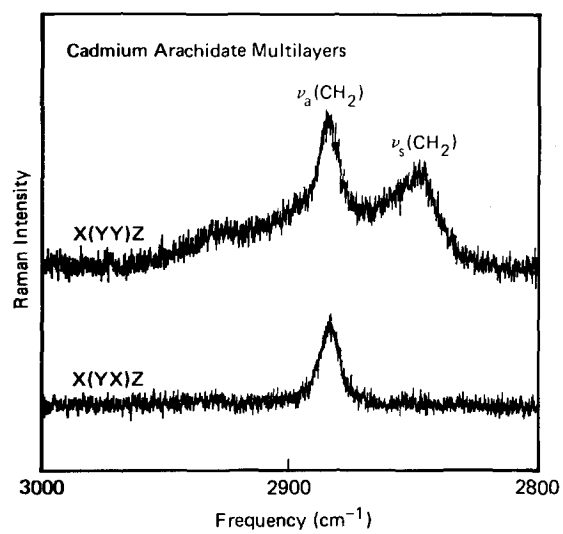

FIG. 4. Polarized Raman spectra of CdA multilayers of CdA in the CH stretching region.

the spectrometer). This would require careful polishing of the sample face perpendicular to the chain axes so as to minimize polarization scrambling. Thus the WRS scattering geometry will give different Raman scattering intensities for the bands associated with the CH_2 groups than is normally observed in more conventional scattering geometries: Now different polarizability derivatives will contribute to the overall scattering intensities. This will become evident in the analyses of the spectra shown in Figs. 3 and 4. It is, perhaps, easiest to begin with the CH stretching region shown in Fig. 4. In the $X(YX)Z$ spectrum, only bands attributable to the A_g and B_{1g} species should be observed. As seen, only the $\nu_a(CH_2)$ band is observed which is known to have B_{1g} symmetry.[19] No A_g band attributable to the $\nu_s(CH_2)$ vibration is found. A better insight into the lack of intensity of the A_g mode in this polarization experiment comes upon consideration of the contribution of the polarizability derivatives to the scattering intensity. In the $X(YX)Z$ experiment the total intensity of A_g modes is proportional to $(\alpha_{xx} - \alpha_{yy})^2$ suggesting that $\alpha_{xx} = \alpha_{yy}$ since the A_g mode appears to have zero intensity. This turns out to be a reasonable assumption due to the isotropic orientation of the axes perpendicular to the molecular backbone, i.e., the LB film possesses uniaxial orientation.

The $X(YY)Z$ spectrum contains an additional term, $(\alpha_{xx} + \alpha_{yy})^2$, which contributes to the intensity of the A_g modes and thus, even if $\alpha_{xx} = \alpha_{yy}$, a nonzero intensity of A_g modes is expected. As shown in Fig. 4, the A_g $\nu_s(CH_2)$ mode is, in fact, observed. In addition, a weaker band located at 2933 cm^{-1}, thought[19] to originate from Fermi resonance interaction between an overtone of a CH_2 bending vibration and $\nu_s(CH_2)$, also exhibits A_g symmetry as it should.

Extending this analysis ot the 1600–800 cm^{-1} region, it becomes apparent from the previous discussion that the $X(YX)Z$ spectrum of Fig. 3 should contain bands of the B_{1g} symmetry species. Correspondingly, both the 1440 and 1460 cm^{-1} bands are assignable to the B_{1g} symmetry species. Interestingly enough, these bands are not visible in the $X(YY)Z$ spectrum as would be expected. In fact, no bands attributable to CdA appear in the top spectrum of Fig. 3. One possible explanation is that the intensity of the background signal from the guiding layer of Corning 7059 glass dominates the spectrum. The broad intense features shown in the $X(YY)Z$ spectrum are approximately four times larger in intensity than the other spectra shown. With this overwhelming signal, the presence of any Raman bands is almost certainly obscured as is the case of bands in the presence of a high fluorescent background. However, although the $X(YY)Z$ spectrum does not provide any new information pertinent to the symmetry analysis, it does indicate the shape of the background present in this region. It should be noted that in the CH stretch region (Fig. 4) no remnants of this background persist and, as discussed previously, the CH stretching vibrations are observed.

Under the D_{2h} symmetry analysis[24] both the $X(ZY)Z$ and the $X(ZX)Z$ spectra should be identical and contain bands belonging to the B_{2g} and the B_{3g} symmetry species. As shown in Fig. 3, two bands, the 1295 cm^{-1} $t(CH_2)$ and the 1060 cm^{-1} $\nu_a(CC)$, show up in both spectra with identical intensity as predicted. Although it is impossible to discriminate between B_{2g} and B_{3g} modes from these particular polarization measurements, previous studies on n-paraffins[21] and PE[20] indicate that the 1295 and 1060 cm^{-1} bands can be assigned to the B_{3g} and the B_{2g} symmetry species, respectively. Hence, this is consistent with what is predicted by D_{2h} for the $X(ZY)Z$ and the $X(ZX)Z$ spectra.

Careful inspection of the 1400 cm^{-1} region in the lower two spectra of Fig. 3 indicates the presence of two very weak bands in the vicinity of 1450 cm^{-1} thought to be residual intensity of the 1440 and 1460 cm^{-1} bands observed in the $X(YX)Z$ spectrum. Although this could easily be attributed to disorder and/or defects in the LB film, a more plausible explanation results from consideration of the input polarization for a TM mode of the waveguide. As shown in Fig. 1, the light coupled into the guiding layer undergoes total internal reflection as it propagates down the guide. In a TM configuration, the electric field vector of the incoming light is parallel to the plane formed by the incident and scattered beam. Thus, E is not normal to the waveguide surface but inclined at a small angle (5°–7°). The result of this slight tilt is manifested by the "leaking" of weak bands attributable to other polarizations into both the $X(ZY)Z$ and $X(ZX)Z$ spectra.

An interesting observation can be made by comparing Figs. 2 and 3. Of all the strong bands observed in bulk CdA, only the $\nu_s(CC)$ at 1130 cm^{-1} does not show up in the polarized Raman measurements. This can be understood upon considering the polarizability contribution to its intensity. Because $\nu_s(CC)$ involves the symmetric stretching of CC bonds, the change in polarizability associated with this mode is entirely along the molecular axis.[18–20] Hence α_{zz} is responsible for the mode intensity and, as indicated previously in the symmetry analysis, none of the experiments shown in Fig. 3 provides access to Raman bands whose intensity arises from α_{zz}. The $\nu_s(CC)$ mode could be observed by selection of a different scattering geometry or by the excitation of Raman scattering by surface plasmons[15,25,30] which inherently gives information on this polarizability component.

Based on the successful explanation of the data shown in Figs. 3 and 4 by a D_{2h} symmetry analysis and previous re-

TABLE I. Symmetry assignments of LB films of CdA.

Frequency (cm^{-1})	Assignment[a]	Symmetry species
2933	$\nu_s(CH_2) + \delta(CH_2)$ overtone in Fermi resonance	A_g
2880	$\nu_a(CH_2)$	B_{1g}
2850	$\nu_s(CH_2)$	A_g
1460	$\delta(CH_2)$	B_{1g}
1440	$\delta(CH_2)$	B_{1g}
1415	Fermi resonance of $\delta(CH_2)$ with overtone of $r(CH_2)$	A_g
1295	$t(CH_2)$	B_{3g}
1130	$\nu_s(CC)$	A_g
1060	$\nu_a(CC)$	B_{2g}

[a] Symbols same as in Fig. 2; r—rock.

sults[11] from IR measurements, it is reasonable to conclude that the hydrocarbon tails are oriented almost normal to the surface and are packed into an orthorhombic subcell similar to polyethylene.

C. Elevated temperature measurements

While the polarization dependence of the Raman spectra indicated that the orientation and crystal packing in the LB film is apparently the same on the glass waveguide as was found on silver substrates from infrared experiments, it is the relative intensities and bandwidths which give additional insight into conformational disordering and molecular motion.[26–28] The CH stretch region has been used previously to characterize molecular order in bilayers[29] and LB films[30] and dramatic changes are found upon heating the LB multilayers of CdA towards the phase transition temperature at 110° as shown in Fig. 5. While the $\nu_a(CH_2)$ band at 2880 cm^{-1} broadens slightly asymmetrically with a high frequency shoulder and loses intensity until it disappears around 100°, the $\nu_s(CH_2)$ band at 2850 cm^{-1} remains fairly constant. One also observes that the band around 2930 cm^{-1} grows relative to the 2850 cm^{-1} band.

The broadening of the 2880 cm^{-1} band has been attributed to a change in intermolecular environment[19,26–28] with temperature. In the case of the LB film of CdA this would mean an increase in hindered rotation (libration) about the molecular axis since the carboxylate head group serves as an "anchor" fixing at least one end of the hydrocarbon chain. An interesting comparison results when the CH stretching region of the CdA bulk sample is considered (Fig. 6). As shown, similar broadening of the $\nu_a(CH_2)$ and $\nu_s(CH_2)$ bands occur with temperature but it appears that the onset of molecular mobility occurs in the range of 110 °C, about 10 °C higher than that observed for the LB film. This temperature difference is larger than the experimental error found by measuring the temperature of the waveguide at the exact point of sampling and thus suggests that this lag in the onset of molecular mobility in bulk CdA may be associated with a different packing of hydrocarbon chains.

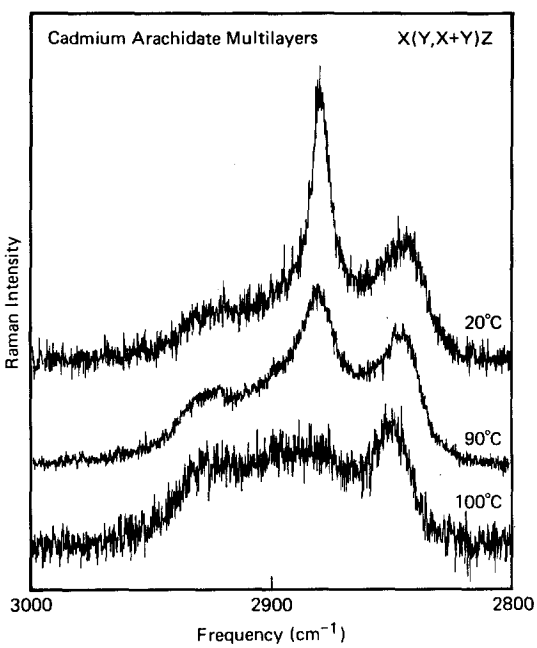

FIG. 5. Polarized Raman measurements (3000–2800 cm^{-1}) of CdA multilayers as a function of temperature. Although input light is polarized in Y direction, both the X and Y components of the scattered light are detected simultaneously, i.e., no analyzer is used in this measurement.

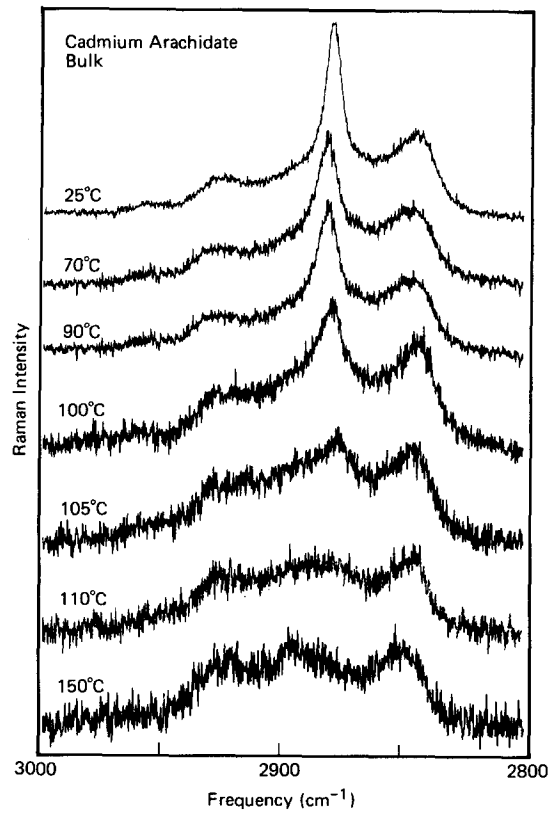

FIG. 6. Raman spectra in the 2800–3000 cm^{-1} region of bulk CdA as a function of temperature. The bottom four spectra have been expanded by 2× so as to facilitate comparison.

Another contribution to the broadening of $\nu_a(CH_2)$ could originate from the introduction of *gauche* defects into the *trans* planar chain.[26–29] As shown in Fig. 7 (LB film) and Fig. 8 (bulk) no large scale introduction of *gauche* bonds is observed since significant growth of a 1080 cm^{-1} *gauche* band does not occur with temperature. In previous work[29] on phospholipids, a band at 1080 cm^{-1} dominated the spectrum in this region when the all *trans* hydrocarbon chain was raised to higher temperatures. Certainly, this is not the case in either Fig. 7 or 8 although some high frequency asymmetry is observed for the 1060 cm^{-1} ν_a (CC) band in both cases as the temperature approaches the 80–90 °C range.

From Figs. 7 and 8 it is quite clear that the ν_a (CC) band loses intensity as the temperature increases towards 100 °C while the 1080 cm^{-1} shoulder becomes more pronounced, indicating a rapid increase in the concentration of *gauche* bonds. This is what would be expected for the onset of an order–disorder transition which is known to occur in this temperature region. It should be further noted that ellipsometric determination[31] of the aerial mass density of an LB film of CdA as a function of temperature indicated that the

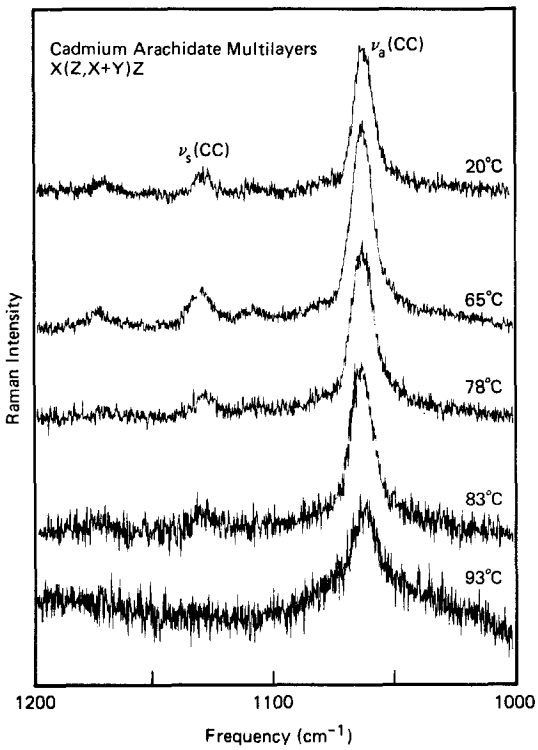

FIG. 7. Polarized Raman measurements of CC stretching region of CdA multilayers as a function of temperature. ν_s—symmetric stretch; ν_a—asymmetric stretch.

additional space needed for the hydrocarbon chains to disorder results from the creation of voids due to the ablation of chain molecules from the monolayer.

IV. CONCLUSIONS

Polarized Raman measurements of Langmuir–Blodgett films of CdA have been obtained using integrated optical techniques. Symmetry analysis of the observed spectra indicate that the hydrocarbon tails are oriented normal to the surface as would be expected for the salt of a fatty acid.[11] Infrared measurements[12] showed that chain disorder starts occurring around 65 °C while the head group remained oriented up to the "melting" temperature (110 °C). Raman measurements reported here, on the other hand, show a beginning evidence for *gauche* defects only above 90 °C. Therefore, the increased chain mobility and disorder between 65 and 90 °C must be a result of chain tilting, probably near voids and vacancies. Similar observations were made for bulk CdA with the noted exception that the onset of motion and disorder occurred at a slightly higher temperature than that found in LB films. This suggested that a denser packing of hydrocarbon chains exists in bulk CdA than in LB films of CdA perhaps due to the additional packing constraints in 3D crystals.

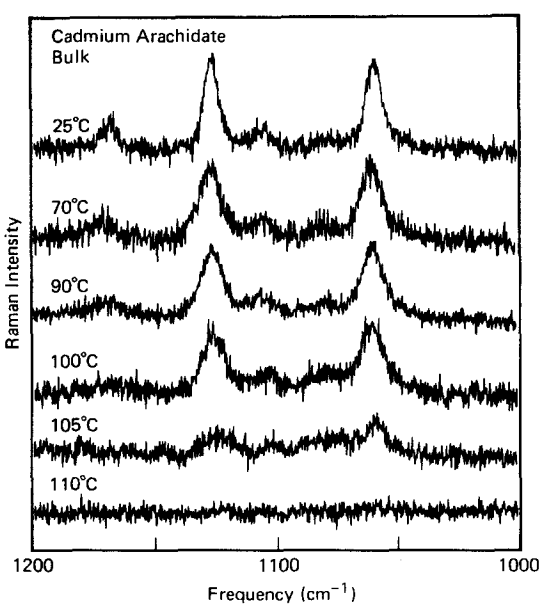

FIG. 8. Raman measurements of bulk CdA in the CC stretching region as a function of temperature.

ACKNOWLEDGMENTS

It is a pleasure to acknowledge the help of Jennifer S. Green and Charles Naselli with sample preparation and some of the Raman measurements.

[1]Y. Levy, C. Imbert, J. Cipriani, S. Racine, and R. Dupeyrat, Opt. Commun. **11**, 66 (1974).
[2]Y. Levy and R. Dupeyrat, J. Phy. Colloque C5 **38**, 253 (1977).
[3]J. F. Rabolt, R. Santo, and J. D. Swalen, Appl. Spectrosc. **33**, 549 (1979).
[4]J. F. Rabolt, R. Santo, and J. D. Swalen, Appl. Spectrosc. **34**, 517 (1980).
[5]J. D. Swalen and J. F. Rabolt, in *Vibration at Surfaces*, edited by R. Caudano, J. M. Giles, and A. A. Lucas (Plenum, New York, 1982), pp. 413–420.
[6]J. F. Rabolt and J. D. Swalen, in *Advances in Spectroscopy Series: Spectroscopy of Surfaces*, edited by R. Clarke and R. Hester (Wiley, London, 1987).
[7]E. Barbaczy, F. Dodge, and J. F. Rabolt, Appl. Spectrosc. (in press).
[8]J. F. Rabolt, R. Santo, N. E. Schlotter, and J. D. Swalen, IBM J. Res. Dev. **26**, 209 (1982).
[9]J. F. Rabolt, N. E. Schlotter, and J. D. Swalen, J. Phys. Chem. **85**, 4141 (1981).
[10]See Thin Solid Films, Vols. 132–134 (1985).
[11]J. F. Rabolt, F. C. Burns, N. E. Schlotter, and J. D. Swalen, J. Chem. Phys. **78**, 946 (1983).
[12]C. Naselli, J. F. Rabolt, and J. D. Swalen, J. Chem. Phys. **82**, 2136 (1985).
[13]D. L. Allara and J. D. Swalen, J. Phys. Chem. **86**, 2700 (1982).
[14]W. G. Golden, C. D. Snyder, and B. Smith, J. Phys. Chem. **86**, 4675 (1982).
[15]W. Knoll, M. R. Philpott, J. D. Swalen, and A. Girlando, J. Chem. Phys. **77**, 2254 (1982).
[16]D. Saperstein and W. Golden, ACS Preprints, August 1984.
[17]P. P. A. Spegt and A. E. Skoulios, Acta Crystallogr. **16**, 301 (1963).
[18]R. G. Snyder, J. Mol. Spectrosc. **4**, 411 (1960).
[19]R. G. Snyder, S. L. Hsu, and S. Krimm, Spectrochim. Acta Part A **34**, 395 (1978).
[20]G. Masetti, S. Abbate, M. Gussoni, and G. Zerbi, J. Chem. Phys. **73**, 4671 (1980).
[21]P. J. Hendra, H. P. Jobic, E. P. Marsden, and D. Bloor, Spectrochim. Acta Part A **33**, 445 (1977).
[22]T. C. Damen, S. P. S. Porto, and B. Tell, Phys. Rev. **142**, 570 (1966).
[23]M. Prakash, P. Dutta, J. B. Ketterson, and B. M. Abraham, Chem. Phys. Lett. **111**, 395 (1984).

[24]R. G. Snyder, J. Mol. Spectrosc. **37**, 353 (1971).
[25]M. Masson, M. Caillaud, P. Zhi-nan, and R. Dupeyrat, Opt. Commun. **53**, 33 (1985).
[26]Y. Cho, M. Kobayashi, and H. Tadokoro, J. Chem. Phys. **84**, 4636 (1986).
[27]Y. Cho, M. Kobayashi, and H. Tadokoro, J. Chem. Phys. **84**, 4643 (1986).
[28]S. L. Wunder, M. Bell, and G. Zerbi, J. Chem. Phys. (in press).
[29]B. P. Gaber and W. Peticolas, Biochim. Biophys. Acta **465**, 260 (1977).
[30]W. Knoll, J. Rabe, M. R. Philpott, and J. D. Swalen, Thin Solid Films **99**, 173 (1983).
[31]J. P. Rabe, J. F. Rabolt, and V. Novotny (to be published).